

An Energy-Efficient Spiking Neural Network for Finger Velocity Decoding for Implantable Brain-Machine Interface

Jiawei Liao^{*†}, Lars Widmer[†], Xiaying Wang[†], Alfio Di Mauro[†], Samuel R. Nason-Tomaszewski[‡],
Cynthia A. Chestek[‡], Luca Benini[†], Taekwang Jang[†]
ETH Zurich, Switzerland[†] University of Michigan, USA[‡] *Email: liaoj@iis.ee.ethz.ch

Abstract—Brain-machine interfaces (BMIs) are promising for motor rehabilitation and mobility augmentation. High-accuracy and low-power algorithms are required to achieve implantable BMI systems. In this paper, we propose a novel spiking neural network (SNN) decoder for implantable BMI regression tasks. The SNN is trained with enhanced spatio-temporal backpropagation to fully leverage its ability in handling temporal problems. The proposed SNN decoder achieves the same level of correlation coefficient as the state-of-the-art ANN decoder in offline finger velocity decoding tasks, while it requires only 6.8% of the computation operations and 9.4% of the memory access.

Index Terms—Brain-machine interface, motor decoding, spiking neural network, spatio-temporal backpropagation

I. INTRODUCTION

Brain-machine interfaces (BMIs) acquire signals generated by neurons, use them to decode users' intentions, and convert them into commands that can be used to control actuators like robotic arms and prostheses. They are essential tools in motor rehabilitation by restoring the movement ability of amputees and tetraplegic patients [1]–[4].

To achieve the objective, it is essential to develop accurate algorithms to decode motor function from neural signals. Linear decoders, including linear regression [2], linear discriminant analysis [4], and variants of Kalman filters [1], [3], [5] have been developed to perform arm and hand control. To further improve the accuracy, nonlinear decoders such as recurrent neural network [6], [7] and feed forward neural network [8], [9] are actively investigated. While neural networks are powerful, they come at the cost of high computational complexity, implying high energy consumption in hardware implementation [10]. For BMIs, that perform their inference tasks in the implanted devices to reduce the wireless communication overhead for the large volumes of raw data, their power efficiency is a critical concern to limit the heat generation and to protect the surrounding tissues. As a result, highly energy efficient approaches, that match the accuracy achieved by artificial neural network (ANN) should be designed.

Spiking neural networks (SNNs), a computing paradigm inspired by biological neural networks, have potential for achieving energy-efficient computation by leveraging sparsity introduced by the asynchronous feature of the neurons [11]. While SNNs have been heavily studied to solve classification

tasks [12], [13], they are perfect candidates for solving regression tasks with spatio-temporal inputs and outputs, such as motor decoding, thanks to their nature of taking time series as input and generating time series output.

There are three main ways to construct SNNs: 1) The first is ANN-to-SNN conversion. This requires an ANN trained before being converted to the SNN. Typically, it relies on rate coding and tries to mimic the computation of the ANN by setting the parameters of the SNN to correlate the spiking neurons' firing rates with the neurons' activation of the original ANN [14]. This conversion approach has shown similar performance as its ANN counterparts. 2) The second is unsupervised learning such as spike-timing-dependent-plasticity (STDP). This is a biologically plausible approach relying on local learning rules [15]. However, without global supervision, so far, it has not achieved state-of-the-art performance in terms of accuracy and energy efficiency. 3) The third is SNN backpropagation such as spatio-temporal-back-propagation (STBP) [12], [13]. By applying a surrogate function in the backward flow to approximate the derivative of the spike activity, the error backpropagation path can be established for gradient descent training. This approach utilizes the temporal feature of the input and has demonstrated good performance in classification tasks. In this work, we construct the SNN using the SNN backpropagation method.

In this paper, we propose a novel low-complexity SNN trained with improved STBP backpropagation method to predict the open-loop two-finger velocities for implantable BMIs. The main contributions are:

- We propose and open source¹ a novel low-complexity SNN based on leaky-integrated-and-fire (LIF) neurons for regressing continuous-time finger velocity decoding for low-power implantable BMIs.
- We demonstrate that the STBP SNN training strategy can be enhanced with techniques such as the neuron reset-by-subtraction scheme and trainable decay factors to achieve the same level of performance as a state-of-the-art ANN decoder.
- We validate the accuracy of the proposed SNN on two datasets recorded from non-human primates' hand area of

¹<https://github.com/liaoRichard/SNN-for-Finger-Velocity-iBMI>

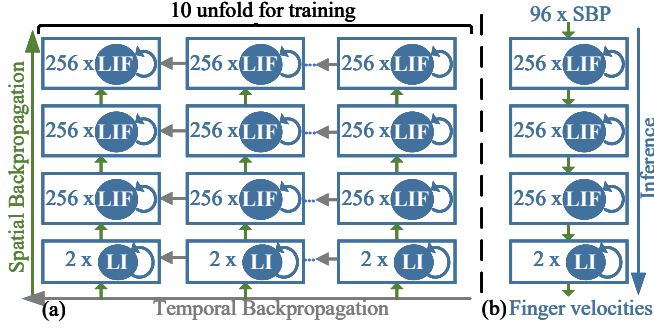


Fig. 1: Proposed SNN unfolded for training (a) and in inference (b)

primary motor cortex for open-loop decoding tasks with two individual finger groups, in a streaming fashion, to mimic a real-time decoding scenario.

- We perform an SNN computation complexity analysis and compare it with both the state-of-the-art ANN decoder and the ANN-converted SNN. The proposed SNN requires only 6.8% computation operations and 9.4% memory access compared to the ANN, indicating its potential for more energy-efficient hardware implementation.

II. METHODS

A. Neuron model

We use the adjusted LIF neuron model for its simplicity in hardware implementation [16]. As demonstrated in [16], the LIF neuron model shows a good trade-off between cognitive capabilities and computational complexity, making it a suitable candidate for the implementation on embedded platforms with constrained-resources. The implemented neuron model is described in (1), (2), and (3).

$$u^l(t) = \tau(u^l(t-1) - s^l(t-1)V_{th}) + I^l(t) \quad (1)$$

$$I(t) = \sum_{i=0}^{M-1} w^i s^{l-1}(t) \quad (2)$$

$$s^l(t) = \begin{cases} 1 & u^l(t) \geq V_{th} \\ 0 & u^l(t) < V_{th} \end{cases} \quad (3)$$

In (1), u^l represents the membrane potential in l th layer and I represents the input current expressed by (2). V_{th} denotes the threshold voltage of the neuron. M is the number of input connections of the neuron. s is the status of the spike defined by (3) and s equals one when the neuron fires. τ is the decay factor of the leaky neuron. The LIF integrates the input current and leaks at a rate of τ . When the membrane potential exceeds the threshold voltage, the neuron fires and the membrane potential decreases by V_{th} . Inspired by [17], we apply reset-by-subtract scheme instead of reset-by-zero scheme to avoid loss due to the over adjustment after spiking.

B. Network architecture

We use spiking band power (SBP) proposed in [18] as the input to the network. SBP is a neural feature for motor prediction defined as an average of absolute 300–1000 Hz

band-pass-filtered signal. The proposed network handles the SBP features averaged in time frames from 96 channels.

Our proposed SNN architecture is depicted in Fig. 1. It consists of four fully connected layers inspired by [9]. Unlike [9], where the authors use a convolutional layer as the input layer to capture the temporal information from multiple time frames, our network directly receives the features from a single time frame as input. This choice has been made to exploit an intrinsic property of SNNs, i.e., the membrane potential of each neuron acts as a memory element, and stores temporal information from previous inputs. The output layer uses two non-spiking neurons that follow the membrane equation $u(t) = \tau u(t-1) + I(t)$. The membrane voltages $u(t)$ are then taken directly as the continuous-valued outputs for the prediction of two finger velocities for every input.

Except for the first layer of the network whose input current is the weighted sum of the SBP features, in all hidden layers, the total input current I of each LIF neuron is obtained as the weighted sum of the input spikes whose values are either 1 or 0, as described in (2) and (3). Therefore, one of the advantages of using an SNN instead of a conventional ANN is that the input current I can be calculated as additions of weights instead of Multiply-Accumulate (MAC) operations thanks to the 1-bit binary input spikes. Except for the last output layer, all hidden neurons fire only when the membrane potentials exceed the threshold, introducing a high degree of sparsity in the intermediate features. The reduced computational complexity as well as the high degree of sparsity are the two main sources of efficiency of the proposed SNN compared to a conventional ANN.

Between successive layers, the batch normalization is implemented to improve convergence. To handle the extra temporal dimension in SNN and to avoid both gradient vanishing and gradient explosion problems by balancing the firing rate, we use the special threshold-based batch normalization introduced in [13]. Dropout is implemented for regularization during training. The dropout is performed for only spatial dimensions. At each time step, a new dropout mask is generated randomly.

C. Training methods

Spiking functions for neurons in SNNs are not directly differentiable, so this has been an obstacle for direct back-propagation for SNNs for a long time. As suggested by [12], [19], using a surrogate function to approximate the derivative of spike activity allows the gradient to propagate back through the neurons. In this work, we use a square surrogate function defined by (4).

$$\frac{\partial a}{\partial u} = \begin{cases} 1 & \text{if } |u(t) - V_{th}| < 0.5 \\ 0 & \text{else} \end{cases} \quad (4)$$

The training process is based on the publicly available PyTorch implementation of the STBP training method introduced in [12]. The support for reset-by-subtract scheme, trainable decay factor, as well as non-spiking output layers were implemented additionally to the training framework. Instead of defining a decaying factor τ as a hyperparameter

shared by all the neurons, we make it a trainable parameter for each neuron, and optimize them at training time; the value for τ is clamped between 0 and 1 during the forward pass. With different decaying factors, each neuron has an independent behavior when receiving the input spikes, thereby showing a different sensitivity to the events received in the past; this feature increases the expressiveness of the SNN [20], [21].

Fig. 1a shows the unfolded network during the training process. The STBP allows backpropagation through both temporal and spatial dimensions. The network is unfolded for ten time frames during the training process. We experimentally observed that using more than ten frames does not improve the accuracy of the network, therefore, we used ten time-frames as the upper bound of our exploration. Additionally, we discarded the first two frames in the loss calculation, because the network has not yet converged to a stable prediction. The loss is then backpropagated through spatial and temporal dimension in this unfolded network. By using a sliding window whose length is 10 time frames and overlap is 9 time frames, training samples are generated. These samples containing 10 time frames are then shuffled for training.

During the inference process, the network is not unfolded, and all neurons maintain and update their internal state through the whole process. One time frame is used once per inference. This operating scenario mimics the situation where a real-time prediction task runs on data that are streamed continuously to the network. We applied AdamW optimizer [22] with learning rate and weight decay of 2×10^{-3} and 1×10^{-2} , respectively. The batch size used during training is 128. The membrane threshold V_{th} is set to 0.4. These hyperparameters are determined by grid search. Similarly to [9], we use the time-integrated mean square error as the loss function during training while Pearson correlation coefficient is used as the metric to evaluate the performance of SNN as it is commonly used for neural decoding algorithm comparison [9], [18].

III. RESULTS AND DISCUSSION

A. Dataset

We evaluated the proposed SNN on two datasets recorded from non-human primates while they were performing two-degree-of-freedom finger tasks. The datasets contain positions, velocities of two fingers, and the SBP features from 96 channels. Dataset A, also used in [9], contains 817s data. Dataset B is the open-source dataset also used for [5], containing 610s data. The first 80% of the data are used for training, the remaining 20% are for validation. The SNN is trained for 24 epochs and 23 epochs for the evaluation on Dataset A and B respectively. The velocities and SBP features are averaged within time frames to be processed. Time frames' sizes are chosen to be 50ms and 32ms as introduced in [5], [9]. Averaged SBP features are standardized by removing means and scaling to standard deviation of 1 before being fed into the SNN. Predicted velocity is also standardized with statistics from training set. Standardized data are recovered to original scale for inference. An inference is performed for every time frame to generate two finger velocities in a streaming fashion.

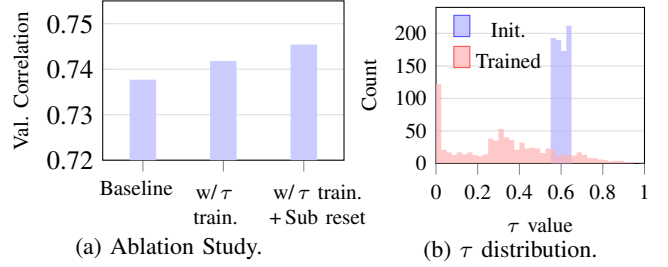


Fig. 2: Ablation study and τ distribution

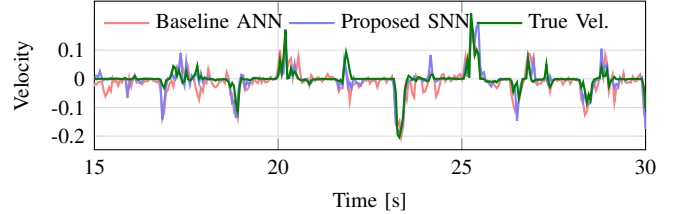


Fig. 3: Example of predicted and true velocities.

B. Performance comparison

The improvements that are achieved by using the proposed trainable decay factor and reset-by-subtract are quantified by the ablation study performed with dataset A and the results are depicted in Fig. 2a. Trainable decay factor and reset-by-subtract scheme jointly improve the correlation coefficient to over 0.74. Fig. 2b shows the decay factors' distribution before and after training for each layer. The trained decay factors cover a wide range of values, allowing different neuron dynamics, which may improve the expressiveness of the network, as suggested by [20].

The results from our SNN experiments are summarized in Table I. For comparison, we reproduced the KF predictor [5] and the NN predictor [9] using the same parameters reported in the original papers. We also compare with the SNN converted from the ANN using SNN toolbox [14]. The proposed network reaches better correlation coefficients than linear KF and achieves the same level of performance as the state-of-the-art ANN decoder. The velocity predicted by the proposed SNN, ANN, and the true velocity of one of the fingers are plotted in Fig. 3 and it shows a good match.

C. Computation complexity analysis

SNNs are appealing for their potentials in achieving efficient hardware implementation [11]. One primary source of

TABLE I: Performance comparison.

Dataset	A	B
KF [5]	0.601	0.459
ANN [9]	0.724 [†]	0.582
Converted SNN	0.740	0.590
Proposed SNN	0.745	0.582

[†] Reproduced.

TABLE II: Operation comparison.

Operation	ANN [9]	Convert. SNN	Prop. SNN
MAC	529K	5K	25K
ADD	-	865K	33K
Total ops [†]	529K	293K	36K
Mem access	2116K	2615K	199K

[†] Total MAC operations. 3 ADDs count as 1 MAC [23].

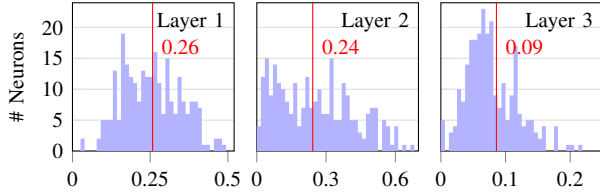


Fig. 4: Spike rate for three spiking layers. Red line shows the average spike rate

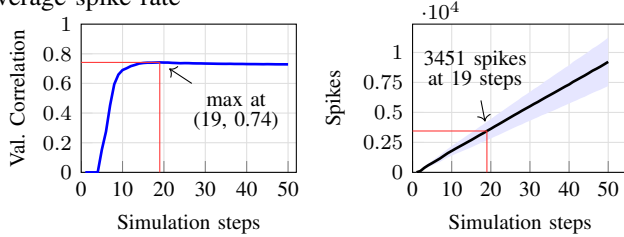


Fig. 5: ANN converted SNN.

efficiency is sparsity. We evaluated the spike rate for neurons in different layers and average spike count in each layer to quantify the sparsity in our network. The results are presented in Fig. 4. Most of the neurons in the all layers have spiking probability well below 50%. The average spike rates are 26%, 24%, 9% for the three spiking layers respectively. In each inference, out of the 770 neurons in the whole network, there are 150 spikes generated on average. Due to the rate approximation, the SNN converted from ANN requires multiple simulation steps on the same input for one output to achieve sufficient accuracy, in this case 19 steps for one prediction. In total, around 3000 spikes are used per inference as shown in Fig. 5. The ANN-converted SNN uses 20 times more spikes than the proposed one, indicating longer latency and higher energy consumption in hardware implementation.

In conventional ANNs, the weighted sum computation for each input to a neuron requires a MAC operation. Whereas in the proposed SNN, as the spike status is either 1 or 0, this process has been replaced by addition operations, which requires much less power [23]. Here, we conservatively assume three additions as one MAC operation according to the ratio of the energy cost for floating point operations reported in [23] for the comparison of the total number of operations. To have a fair comparison between the proposed SNN and ANN, it is important to remark that the SNN needs to update its membrane potentials as described in (1) once per inference, this amounts to an additional MAC operation per each neuron. In this comparison, three memory loads and one store are assumed for each MAC while two loads and one store are assumed for each addition. The average spike rates in Fig. 4 are used for the analysis. Additions and the corresponding memory accesses are not executed when there is no spike. The results are summarized in Table II. Thanks to enhanced STBP training and the high level of sparsity, the proposed SNN requires 6.8% operations and 9.4% memory access compared to the ANN while achieving same level of accuracy.

IV. CONCLUSION

In this paper, we present a spiking neural network and its training method to decode continuous-valued finger velocities

for implantable BMI applications. The proposed network is trained with STBP backpropagation enhanced by trainable decay factor and reset-by-subtract techniques to improve the accuracy while keeping low computation complexity. We compared the performance of the proposed SNN, Kalman filter, ANN, and SNN converted from ANN on two datasets for open-loop finger decoding tasks. The proposed SNN achieves the same level of correlation coefficient as the state-of-the-art decoders, while showing significantly less spike count than SNN converted from ANN and 6.8% operations and 9.4% memory access compared to the ANN decoder, indicating potential in achieving energy-efficient hardware implementation.

REFERENCES

- [1] A. B. Ajiboye *et al.*, "Restoration of reaching and grasping in a person with tetraplegia through brain-controlled muscle stimulation: a proof-of-concept demonstration," *Lancet*, vol. 389, no. 10081, 2017.
- [2] J. L. Collinger *et al.*, "7 degree-of-freedom neuroprosthetic control by an individual with tetraplegia," *Lancet*, vol. 381, no. 9866, 2013.
- [3] L. R. Hochberg *et al.*, "Reach and grasp by people with tetraplegia using a neurally controlled robotic arm," *Nature*, vol. 485, no. 7398, 2012.
- [4] G. Hoson *et al.*, "Individual finger control of the modular prosthetic limb using high-density electrocorticography in a human subject," *J Neural Eng*, vol. 13, no. 2, p. 026017, 2016.
- [5] S. R. Nason *et al.*, "Real-time linear prediction of simultaneous and independent movements of two finger groups using an intracortical brain-machine interface," *Neuron*, vol. 109, no. 19, 2021.
- [6] D. Sussillo *et al.*, "A recurrent neural network for closed-loop intracortical brain-machine interface decoders," *J. Neural Eng.*, 2012.
- [7] T. Hosman *et al.*, "BCI decoder performance comparison of an LSTM recurrent neural network and a kalman filter in retrospective simulation," in *IEEE/EMBS NER*, 2019, pp. 1066–1071, ISSN: 1948-3554.
- [8] J. I. Glaser *et al.*, "Machine learning for neural decoding," *eNeuro*, 2020.
- [9] M. S. Willsey *et al.*, "Real-time brain-machine interface achieves high-velocity prosthetic finger movements using a biologically-inspired neural network decoder," *bioRxiv*, 2021.
- [10] V. Sze *et al.*, "Efficient processing of deep neural networks: A tutorial and survey," *Proceedings of the IEEE*, 2017, proceedings of the IEEE.
- [11] M. Pfeiffer and T. Pfeil, "Deep learning with spiking neurons: Opportunities and challenges," *Frontiers in Neuroscience*, vol. 12, 2018.
- [12] Y. Wu *et al.*, "Spatio-temporal backpropagation for training high-performance spiking neural networks," *Front. Neurosci.*, vol. 0, 2018.
- [13] H. Zheng *et al.*, "Going deeper with directly-trained larger spiking neural networks," *AAAI*, 2021.
- [14] B. Rueckauer *et al.*, "Conversion of continuous-valued deep networks to efficient event-driven networks for image classification," *Front. Neurosci.*, vol. 11, p. 682, 2017.
- [15] T. Masquelier and S. J. Thorpe, "Unsupervised learning of visual features through spike timing dependent plasticity," *PLOS Computational Biology*, vol. 3, no. 2, pp. 1–11, 2007.
- [16] E. Izhikevich, "Which model to use for cortical spiking neurons?" *IEEE Transactions on Neural Networks*, 2004.
- [17] P.-Y. Tan *et al.*, "An improved STBP for training high-accuracy and low-spike-count spiking neural networks," in *DATE*, 2021, pp. 575–580.
- [18] S. R. Nason *et al.*, "A low-power band of neuronal spiking activity dominated by local single units improves the performance of brain-machine interfaces," *Nature Biomedical Engineering*, 2020.
- [19] S. B. Shrestha and G. Orchard, "SLAYER: Spike layer error reassignment in time," in *NeurIPS*, vol. 31, 2018.
- [20] W. Fang *et al.*, "Incorporating learnable membrane time constant to enhance learning of spiking neural networks," in *ICCV*, 2021.
- [21] B. Yin *et al.*, "Accurate and efficient time-domain classification with adaptive spiking recurrent neural networks," *Nature Machine Intelligence*, vol. 3, pp. 905–913, 10 2021.
- [22] I. Loshchilov and F. Hutter, "Decoupled weight decay regularization," in *International Conference on Learning Representations*, 2019.
- [23] M. Horowitz, "1.1 computing's energy problem (and what we can do about it)," in *ISSCC*, 2014.